

## Giant spin splittings in GaSb/AlSb $L$ -valley quantum wells

J.-M. Jancu,<sup>1</sup> R. Scholz,<sup>2</sup> G. C. La Rocca,<sup>1</sup> E. A. de Andrada e Silva,<sup>3</sup> and P. Voisin<sup>4</sup>

<sup>1</sup>*Scuola Normale Superiore and INFM, Piazza dei Cavalieri 7, I-56126 Pisa, Italy*

<sup>2</sup>*Institut für Physik, Technische Universität, D-09107 Chemnitz, Germany*

<sup>3</sup>*Instituto Nacional de Pesquisas Espaciais, Caixa Postal 515, 12201-970 São José dos Campos - São Paulo, Brazil*

<sup>4</sup>*Laboratoire de Photonique et de Nanostructure, CNRS, Route de Nozay, F91000, Marcoussis, France*

(Received 20 July 2004; revised manuscript received 5 August 2004; published 17 September 2004)

For GaSb/AlSb heterostructures with the absolute conduction minimum deriving from the  $L$  point of the bulk Brillouin zone, we predict zero-field spin splittings well exceeding 10 meV, about one order of magnitude larger than typical values resulting from the Dresselhaus and Rashba spin-orbit coupling terms near the zone center. Electronic structure calculations are performed within an improved tight-binding model and the main results can be reproduced in a  $4 \times 4 \mathbf{k} \cdot \mathbf{p}$  Hamiltonian including band parameters and  $k$ -linear spin splittings derived from the GaSb bulk. Our results provide direct insight into  $L$ -valley heterostructures, indicating a promising direction for future research on spintronics.

DOI: 10.1103/PhysRevB.70.121306

PACS number(s): 73.21.Fg, 71.70.Ej, 71.15.Ap, 85.75.-d

Zero-field spin splittings in bulk zinc-blende-type semiconductors due to spin-orbit coupling and to inversion asymmetry have been known for a long time.<sup>1</sup> During the past decade, most studies have been focused on states near the center of the Brillouin zone: close to the  $\Gamma_{6c}$  conduction minimum, the spin splitting induced by bulk inversion asymmetry is of third order in the Cartesian components of the wave vector  $k$ . In heterostructures, additional  $k$ -linear contributions to the electron-spin splitting may originate from mesoscopic inversion asymmetry<sup>2,3</sup> and from microscopic interface asymmetry.<sup>4,5</sup> In GaAs/AlGaAs heterostructures, typical spin splittings are less than 1 meV in the region of  $k$  space occupied by electrons,<sup>6-9</sup> whereas they are typically a few meV in heterostructures based on InAs,<sup>6,7,10-12</sup> which has a much narrower gap. On the other hand, at the  $L$  critical point of the zinc-blende lattice, spin splittings are forbidden along the  $[111]$  direction of the valley axis, but  $k$ -linear splittings are expected on the basis of double-group symmetry considerations<sup>1</sup> for wave vectors transverse to  $[111]$ . Even in nonpolar materials the spin-orbit interaction may lead to a large spin splitting of the  $L$ -derived surface states as observed in Au(111).<sup>13</sup>

Compared to the  $\Gamma$  valley of III-V semiconductors, we predict here much larger spin splittings in the surrounding of the  $L$  point for both bulk and quantum wells (QWs), considering GaSb as prototype material.

The calculations are performed in an  $sp^3d^5s^*$  nearest-neighbor tight-binding (TB) model including spin-orbit coupling<sup>14</sup> with an extremely accurate parametrization, where original parameters have been optimized to fulfill the target of very good agreement with experimental data.<sup>15</sup> The new parametrization was evaluated for suitability in the calculation of spin-orbit coupling effects in the conduction band of GaSb, by comparing model results with *ab initio* calculations.<sup>16,17</sup> In particular, for the directions in  $k$  space available in Ref. 17, we have checked that TB calculations are in very good agreement with fully relativistic linear muffin-tin-orbital results. We first present the spin splittings in bulk GaSb, and then give the results for GaSb/AlSb heterostructures in which the  $L$  valley gives rise to the lowest

electronic subband. In order to rationalize them, a  $\mathbf{k} \cdot \mathbf{p}$  Hamiltonian based on the bulk invariants is constructed for both cases, including intervalley coupling for the quantum well case. To ensure a meaningful comparison, band parameters used in both  $\mathbf{k} \cdot \mathbf{p}$  models (e.g., effective masses and spin-orbit coupling) are set by fitting the TB band structure of bulk GaSb.

Figure 1 shows the zero-field spin splittings in bulk GaSb for the  $\Gamma$  and  $L$  electron valleys together with those of the heavy and light hole bands along the  $[110]$  direction. Defining the size of the spin splitting at a given excess energy with respect to the band extremum as the figure of merit, it is obvious that the transverse directions around the  $L$  point are the most interesting candidates for spintronics applications. However, contrary to those along the  $[110]$  direction,<sup>17</sup> these effects on the surface of the Brillouin zone have not received attention. The spin-dependent Hamiltonian of the conduction band near the  $L$  minimum can be written as

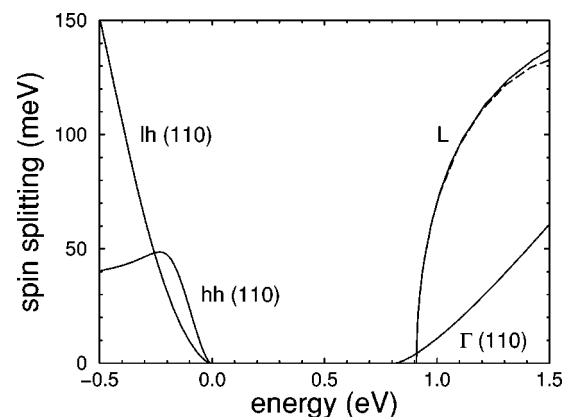


FIG. 1. Calculated zero-field splitting between the two spin states for electrons, heavy holes (hh), and light holes (lh) close to  $\Gamma$ , and for electrons around  $L$  for the directions  $L \rightarrow W$  (solid line) and  $L \rightarrow K$  (dashed line). The spin splittings are reported as a function of the average energy of both spin states.

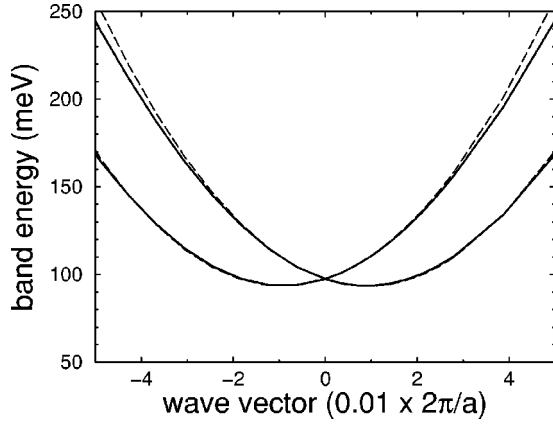


FIG. 2. Dispersion of the two spin states around the  $L$  point in bulk GaSb calculated with a nearest-neighbor  $sp^3d^5s^*$  tight-binding model (solid lines), for  $L \rightarrow K$  (to the left) and  $L \rightarrow W$  (to the right). Coordinates of the zinc-blende points  $L$ ,  $K$ , and  $W$  are, respectively:  $(\frac{1}{2}, \frac{1}{2}, \frac{1}{2})2\pi/a$ ,  $(1, \frac{1}{4}, \frac{1}{4})2\pi/a$ ,  $(1, \frac{1}{2}, 0)2\pi/a$ . The superimposed  $2 \times 2 \mathbf{k} \cdot \mathbf{p}$  model is based on Eq. (1) with  $\alpha=0.84 \text{ eV \AA}$  and a transverse mass of  $m_t=0.087$  (dashed lines). The reference energy is the lowest  $\Gamma_{6c}$  conduction-band state.

$$\begin{aligned}
 H_{(111)} &= \frac{\hbar^2 k_l^2}{2m_l} + \frac{\hbar^2 k_t^2}{2m_t} + \alpha(\mathbf{k} \times \boldsymbol{\sigma}) \cdot \mathbf{n}, \\
 &= \frac{\hbar^2 k_l^2}{2m_l} + \frac{\hbar^2 k_t^2}{2m_t} + \alpha(k_z \sin \theta - k_y \cos \theta)\sigma_x \\
 &\quad + \alpha k_x \sigma_y \cos \theta - \alpha k_x \sigma_z \sin \theta,
 \end{aligned} \quad (1)$$

where  $k_l$  and  $k_t$  are the longitudinal and transverse wave vectors with respect to the  $L$  valley,  $m_l$  and  $m_t$  the band masses along these directions,  $\boldsymbol{\sigma}$  the vector of the  $2 \times 2$  Pauli matrices with the Cartesian components referring to  $\mathbf{e}_x = [1\bar{1}0]/\sqrt{2}$ ,  $\mathbf{e}_y = [110]/\sqrt{2}$ , and  $\mathbf{e}_z = [001]$ , respectively,  $\theta$  the angle between  $[111]$  and  $[001]$ ,  $\mathbf{n} = [111]/\sqrt{3}$  the orientation of the  $L$  valley under study, and  $\alpha$  a material-dependent parameter for the  $k$ -linear spin splitting. The energy-band structure of GaSb along  $L \rightarrow K$  and  $L \rightarrow W$ , where the spin degeneracy is lifted, is shown in Fig. 2 (along the  $L \rightarrow \Gamma$  direction the electronic band remains twofold degenerate). The present calculations give  $\alpha=0.84 \text{ eV \AA}$  for GaSb,<sup>18</sup> corroborated by density-functional results in the local-density approximation,<sup>16</sup> and the resulting  $2 \times 2 \mathbf{k} \cdot \mathbf{p}$  model is superimposed on the tight-binding results in Fig. 2. In the energetic region of interest for the quantized states in a  $L$ -valley quantum well, this  $\mathbf{k} \cdot \mathbf{p}$  model is very precise.

The ideal heterostructure realizing a spin splitting for the lowest quantized conduction states resembling Fig. 2 consists of GaSb quantum wells between AlSb barriers grown along the  $[111]$  direction. As the quantization energy of the states deriving from the  $L$  valley is based on the large longitudinal mass  $m_l=1.3$ , they remain the lowest quantized states up to well thicknesses beyond 19 ML (1 ML= $a/2 \approx 3.06 \text{ \AA}$ ). On the other hand, for technological reasons, a  $[001]$  orientation of the growth axis is preferable. In GaSb/AlSb quantum well heterostructures grown on (001) substrate, the character of the lowest conduction state is

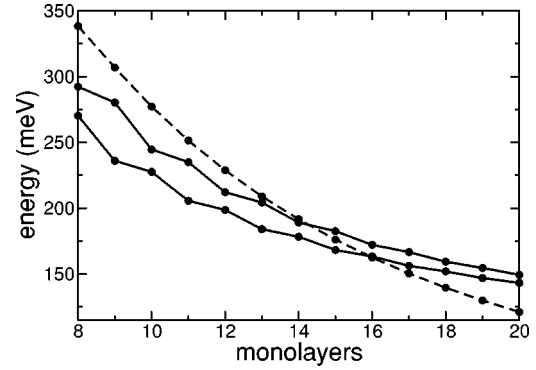


FIG. 3. Tight-binding energy levels vs well thickness (in ML) of  $L$ -like (solid lines) and  $\Gamma$  (dashed line) conduction states in GaSb/AlSb quantum wells lattice matched on GaSb(001). The two  $L$ -derived states at each thickness correspond to states split by the intervalley coupling. The  $L$  band edge offset is 1 eV.<sup>15</sup> The confinement energies are reported with respect to the  $\Gamma_{6c}$  band edge in the well region.

known to change from an  $L$ -derived to a  $\Gamma$ -derived state if the thickness of the well is larger than 14 ML.<sup>19</sup> Further increase in the energy separation between  $L$  and  $\Gamma$  subbands can be achieved by controlling the  $L$ -band-edge positions in the quantum structure, using, for instance, an AlGaSb alloy as well material.<sup>20</sup> These systems are particularly suitable for optical applications based on  $L$ -like intersubband transitions at normal incidence.<sup>20,21</sup>

The calculation of the quantum confined conduction states reported in Fig. 3 reproduces the crossing between direct and indirect minima in the thickness region where it is observed.<sup>19,22</sup> As the two bulk  $L$  valleys at  $(\frac{1}{2}, \frac{1}{2}, \frac{1}{2})2\pi/a$  and  $(\frac{1}{2}, \frac{1}{2}, \frac{1}{2})2\pi/a$  project onto the same wave vector  $(\frac{1}{2}, \frac{1}{2}, 0)2\pi/a$  at the surface of the two-dimensional (2D) Brillouin zone of the heterostructure (2D  $L$  point), states originating from two different regions of the bulk Brillouin zone can mix via the quantum well potential. In a perturbative approach, the leading order of this coupling is proportional to the product of the envelope functions at the interfaces. Symmetry considerations show that the coupling is finite (vanishing to first order) for an odd (even) number of monolayers in the QW region,<sup>23</sup> which leads to pronounced even-odd oscillations in the splitting between the two lowest  $L$ -like states.

Figure 4 shows the spin splittings of the lowest conduction subbands for wave vectors  $\mathbf{k}_{2D}$  in the plane of the 2D Brillouin zone around the 2D  $L$  point. Large zero-field spin splittings occur for all in-plane directions around the quantized states deriving from the  $L$  point of bulk GaSb (see also Fig. 5).

In order to deduce a  $\mathbf{k} \cdot \mathbf{p}$  model including spin for the GaSb quantum well, we start with the effective-mass bulk Hamiltonian [Eq. (1)]. In the following, we first solve for the quantum well confined states without spin,<sup>24</sup> and then derive a  $4 \times 4 \mathbf{k} \cdot \mathbf{p}$  model to deal with spin-orbit coupling via degenerate perturbation theory.<sup>25,26</sup> For simplicity, we assume infinite barriers and vanishing envelope functions at the interfaces  $|z|=l_w/2$ . Without intervalley coupling, the envelope functions for the  $(\frac{1}{2}, \frac{1}{2}, \frac{1}{2})2\pi/a$  and  $(\frac{1}{2}, \frac{1}{2}, \frac{1}{2})2\pi/a$  valleys can be written as

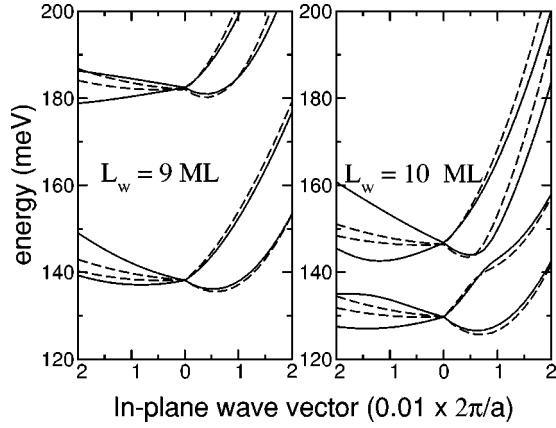


FIG. 4. In-plane dispersion of the lowest  $L$ -conduction subbands, for  $(\text{GaSb})_9(\text{AlSb})_{20}$  (left panel) and  $(\text{GaSb})_{10}(\text{AlSb})_{20}$  (right panel) as a function of  $k_x$  (to the right) and  $k_y$  (to the left), respectively, along the  $[\bar{1}\bar{1}0]$  and  $[110]$  directions. Black solid lines: TB calculation, dashed lines:  $4 \times 4 \mathbf{k} \cdot \mathbf{p}$  model according to Eq. (6) based on the parameters  $m_l=0.087$ ,  $m_t=1.3$ , and  $\alpha=0.84 \text{ eV \AA}$  of bulk GaSb. The quantum confinement energy  $\bar{E}$  and the intervalley couplings  $V$  and  $W$  were set by fitting TB results, resulting in  $\bar{E}=160$ ,  $V=18.5$ , and  $W=11.7 \text{ meV}$  for 9 ML, and  $\bar{E}=138$ ,  $V=3.4$ , and  $W=7.7 \text{ meV}$  for 10 ML. The reference energy is reported with respect to the  $L_{6c}$  band edge in the well region.

$$\psi_{(11\pm 1)} = \frac{e^{ik_x x + ik_y y}}{\sqrt{A}} \sqrt{\frac{2}{l_w}} \cos\left(\frac{\pi}{l_w} z\right) e^{\pm i \phi k_y z}, \quad (2)$$

where the plane-waves  $\exp(\pm i \phi k_y z)$  with

$$\phi = \frac{(m_l - m_t) \cos \theta \sin \theta}{m_t \cos^2 \theta + m_l \sin^2 \theta} \sim 0.64 \quad (3)$$

result from the misorientation of the effective-mass ellipsoid with respect to the growth direction,<sup>24</sup> and the energies of the confined states have a parabolic dispersion,

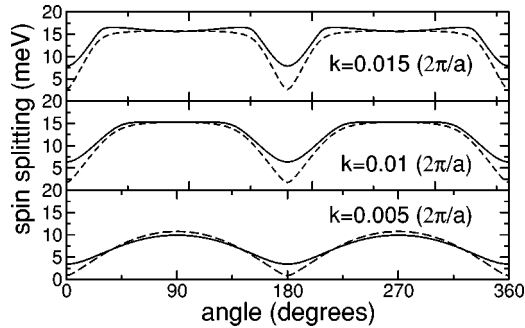


FIG. 5. Spin splitting of the lowest conduction band in a 10-ML GaSb/AlSb quantum well as a function of the angle between the in-plane wave vector  $\mathbf{k}_{2d}$  and the  $[110]$  direction near the  $L$  point. The results of the  $\mathbf{k} \cdot \mathbf{p}$  model in Eq. (7) (dashed lines) are compared with the tight-binding results (solid lines), for different values of  $|\mathbf{k}_{2d}|$  as annotated.

$$E_{2d}(k_x, k_y) = \bar{E} + \frac{\hbar^2 k_x^2}{2m_2} + \frac{\hbar^2 k_y^2}{2m_3} \quad (4)$$

with  $m_3 = m_t \cos^2 \theta + m_l \sin^2 \theta$ ,  $m_2 = m_t$ , while the quantum confinement energy  $\bar{E}$  is considered a fitting parameter.

The two intravalley  $2 \times 2$  blocks accounting for the spin-orbit coupling within each  $L$  valley can be obtained from expectation values of the spin-dependent part of the bulk Hamiltonian Eq. (1) over the envelope functions in Eq. (2) by using  $k_z = -i(\partial/\partial z)$ . Noting that the spin-orbit Hamiltonian for the valley around  $(\frac{1}{2}, \frac{1}{2}, \frac{1}{2})2\pi/a$  turns out to differ from Eq. (1) by the sign of the terms proportional to  $\sin \theta$ , we obtain

$$\langle H_{(11\pm 1)} \rangle = E_{2d}(k_x, k_y) + \alpha[\beta k_y \sigma_x + k_x(\sigma_y \cos \theta \mp \sigma_z \sin \theta)], \quad (5)$$

with  $\beta = \phi \sin \theta - \cos \theta \sim -0.056$ .

In order to describe the intervalley coupling, we phenomenologically introduce two real parameters  $V$  and  $W$ , the latter corresponding to spin mixing induced by the confining potential. Consistent with the  $C_{2v}$  symmetry of the 2D  $L$  point, the resulting  $4 \times 4$  Hamiltonian has the following form:

$$H = \begin{pmatrix} E_{2d} - A & C & V & iW \\ C^* & E_{2d} + A & iW & V \\ V & -iW & E_{2d} + A & C \\ -iW & V & C^* & E_{2d} - A \end{pmatrix}, \quad (6)$$

where  $A = \alpha k_x \sin \theta$  and  $C = \alpha(\beta k_y - i k_x \cos \theta) = |C|e^{i\gamma}$ . The spins are quantized along the  $z$  direction (001), and the different lines refer to the zeroth order states  $\psi_{(111)}|\uparrow\rangle$ ,  $\psi_{(111)}|\downarrow\rangle$ ,  $\psi_{(11\bar{1})}|\uparrow\rangle$ , and  $\psi_{(11\bar{1})}|\downarrow\rangle$ , respectively. The four eigenvalues are given by

$$E = E_{2d}(k_x, k_y) \pm [A^2 + |C|^2 + V^2 + W^2 \pm 2\sqrt{(A^2 + |C|^2)(V^2 + W^2) - (AV + W|C|\sin \gamma)^2}]^{1/2}. \quad (7)$$

In this model the spin splittings do not depend directly on the well thickness, but have a small indirect dependence through the values of  $V$  and  $W$ . As visualized in Fig. 4, the  $\mathbf{k} \cdot \mathbf{p}$  Hamiltonian in Eq. (6) gives a good description of the direction  $k_x \parallel [\bar{1}\bar{1}0]$  based on the GaSb bulk parameters, and intervalley couplings  $V$  and  $W$  chosen in order to ensure the best agreement with TB results. However, along  $k_y$ , the  $k$ -linear spin splittings are underestimated.<sup>27</sup> This difference is examined in more detail in Fig. 5, which shows that the discrepancy is limited to a narrow range of directions close to  $[110]$ . In particular, the large plateaus around  $[\bar{1}\bar{1}0]$  observed in the tight-binding results are well reproduced by the  $\mathbf{k} \cdot \mathbf{p}$  model introduced here, which is the simplest possible one.

In conclusion, we have demonstrated that spin splittings well exceeding 10 meV can be realized in symmetric GaSb/AlSb  $L$ -valley quantum wells. By a careful combination with asymmetries of the confining potential, or by external electric-field gating, additional freedom for the control of the spin properties of the electronic bands could be

achieved. The giant zero-field spin splittings of  $L$ -valley heterostructures point to a promising direction for future research on spin electronics.

The authors thank P. Krüger for unpublished LDA calculations and F. Bassani for clarifying discussions.

- 
- <sup>1</sup>G. Dresselhaus, Phys. Rev. **100**, 580 (1955).  
<sup>2</sup>Yu. A. Bychkov and E. I. Rashba, Sov. Phys. JETP **39**, 78 (1984).  
<sup>3</sup>D. D. Awschalom, D. Loss, and N. Samarth, in *Semiconductor Spintronics and Quantum Computation*, edited by K. von Klitzing, H. Sakaki, and R. Wiesendanger, Nanoscience and Technology Series (Springer, Berlin, 2002).  
<sup>4</sup>O. Krebs and P. Voisin, Phys. Rev. Lett. **77**, 1829 (1996).  
<sup>5</sup>L. Vervoort, R. Ferreira, and P. Voisin, Semicond. Sci. Technol. **14**, 227 (1999).  
<sup>6</sup>E. A. de Andrada e Silva, G. C. La Rocca, and F. Bassani, Phys. Rev. B **50**, 8523 (1994).  
<sup>7</sup>E. A. de Andrada e Silva, G. C. La Rocca, and F. Bassani, Phys. Rev. B **55**, 16293 (1997).  
<sup>8</sup>L. Wissinger, U. Rösler, R. Winkler, B. Jusserand, and D. Richards, Phys. Rev. B **58**, 15375 (1998).  
<sup>9</sup>P. Pfeffer, Phys. Rev. B **59**, 15902 (1999).  
<sup>10</sup>J. Luo, H. Munekata, F. F. Fang, and P. J. Stiles, Phys. Rev. B **41**, 7685 (1990); B. Das, S. Datta, and R. Reifengerger, *ibid.* **41**, 8278 (1990).  
<sup>11</sup>C.-M. Hu, J. Nitta, T. Akazaki, H. Takayanagai, J. Osaka, P. Pfeffer, and W. Zawadzki, Phys. Rev. B **60**, 7736 (1999).  
<sup>12</sup>T. Matsuyama, R. Kürsten, C. Meissner, and U. Merkt, Phys. Rev. B **61**, 15 588 (2000).  
<sup>13</sup>J. Henk, A. Ernst, and P. Bruno, Phys. Rev. B **68**, 165416 (2003).  
<sup>14</sup>J.-M. Jancu, R. Scholz, F. Beltram, and F. Bassani, Phys. Rev. B **57**, 6493 (1998).  
<sup>15</sup>I. Vurgaftman and J. R. Meyer, J. Appl. Phys. **89**, 1 (2001).  
<sup>16</sup>P. Krüger (private communication).  
<sup>17</sup>M. Cardona, N. E. Christensen, and G. Fasol, Phys. Rev. B **38**, 1806 (1988).  
<sup>18</sup>In units of eV Å, the calculated  $k$ -linear terms around the  $L$  conduction minimum of the bulk semiconductors are 0.27 (GaAs), 0.22 (AlAs), 0.10 (InAs), 0.84 (GaSb), 0.51 (AlSb), 0.74 (InSb).  
<sup>19</sup>A. Forchel, U. Cebulla, G. Tränkle, E. Lach, T. L. Reinecke, H. Kroemer, S. Subbanna, and G. Griffiths, Phys. Rev. Lett. **67**, 3217 (1986).  
<sup>20</sup>J.-M. Jancu, F. Bassani, and P. Voisin, J. Appl. Phys. **92**, 641 (2002).  
<sup>21</sup>E. R. Brown, S. J. Eglash, and K. A. McIntosh, Phys. Rev. B **46**, 7244 (1992).  
<sup>22</sup>Deviations from available experimental data are related to the use of the GaSb value for the in-plane lattice constant of the entire heterostructure.  
<sup>23</sup>D. Z.-Y. Ting and Y.-C. Chang, Phys. Rev. B **38**, 3414 (1988).  
<sup>24</sup>F. Stern and W. E. Howard, Phys. Rev. **163**, 816 (1967).  
<sup>25</sup>R. Eppenga and M. F. H. Schuurmans, Phys. Rev. B **37**, 10 923 (1988).  
<sup>26</sup>P. V. Santos, M. Willatzen, M. Cardona, and A. Cantarero, Phys. Rev. B **51**, 5121 (1995).  
<sup>27</sup>By increasing the potential offset at  $L$  artificially, we have found that the tight-binding results come closer to the dispersion obtained from the  $\mathbf{k} \cdot \mathbf{p}$  Hamiltonian, indicating that the deviations at a finite potential offset result from the penetration of the envelopes into the barrier region.